SUPPLEMENTAL MATERIAL

Xi et al., http://www.jem.org/cgi/content/full/jem.20091508/DC1

Generation of CLM-1 KO (−/−) mice. CLM-$1^{+/-}$ embryonic stem cells were generated by electroporating linearized targeting vector DNA into C2 embryonic stem cells of C57BL/6 mice, replacing exon 1 with a neomycin-resistance gene (Neo^r; Fig. S2 A). Neomycin resistant clones were selected and homologous recombination was confirmed by Southern blotting (unpublished data) and PCR. Targeted clones were injected into BALB/C blastocysts to generate male chimeric mice of germline transmission. CLM-$1^{+/-}$ females and males were intercrossed to generate CLM-$1^{-/-}$ mice. For genotyping, a PCR-based strategy using a common sense primer 5′-AAGCACCGAGCCTGCACATT-3′ and a WT-specific (5′-CCACTCCTGCGTCTCCTGGT-3′) and KO-specific (5′-GGACAGCAAGGGGGAGGATT-3′) antisense primer was used, amplifying a 237-bp fragment for the WT allele and a 328-bp fragment for the mutant allele (Fig. S2 B).

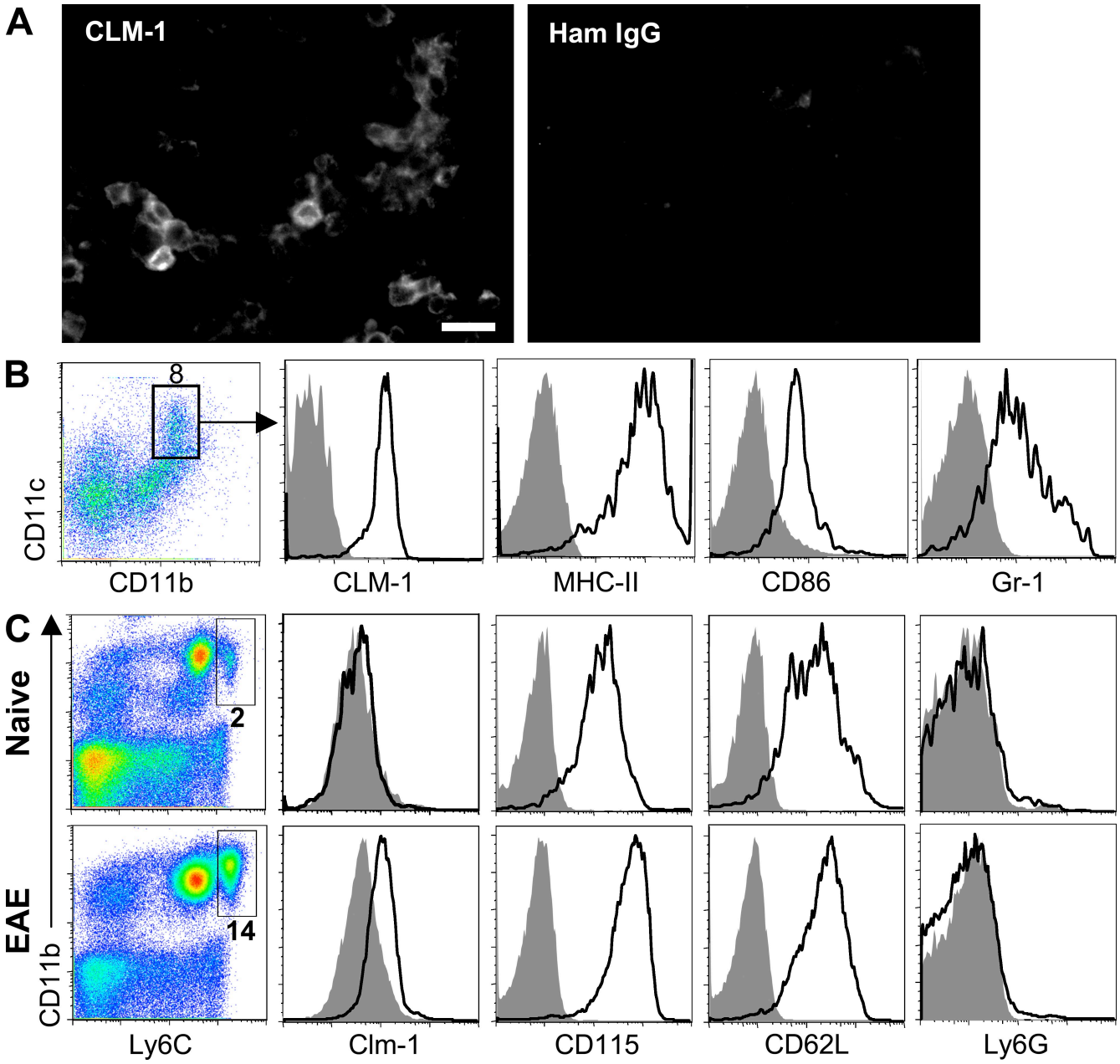

Figure S1. CLM-1 localization on CNS- and blood-resident inflammatory myeloid cells. (A) Sections stained with antibody to CLM-1 and biotinylated hamster IgG as an isotype control for CD11c staining. Bar, 10 µm. (B) CNS inflammatory DCs at peak of EAE express MHC-II, CD86, and Gr-1 as well as CLM-1. Similar results were obtained from three independent experiments. (C) CLM-1 expression on inflammatory monocytes in the peripheral blood during EAE induction. Peripheral blood from day 7 EAE mice was analyzed by FACS for expression of Ly6C, CLM-1, CD115, CD62L, and Ly6G. Inflammatory monocytes were identified as $CD11b^{+}Ly6C^{hi}CD115^{+}CD62L^{+}Ly6G^{-}$. The open histograms show antigen-specific staining and the shaded histograms represent isotype control staining. Results shown represent two experiments with five mice per group.

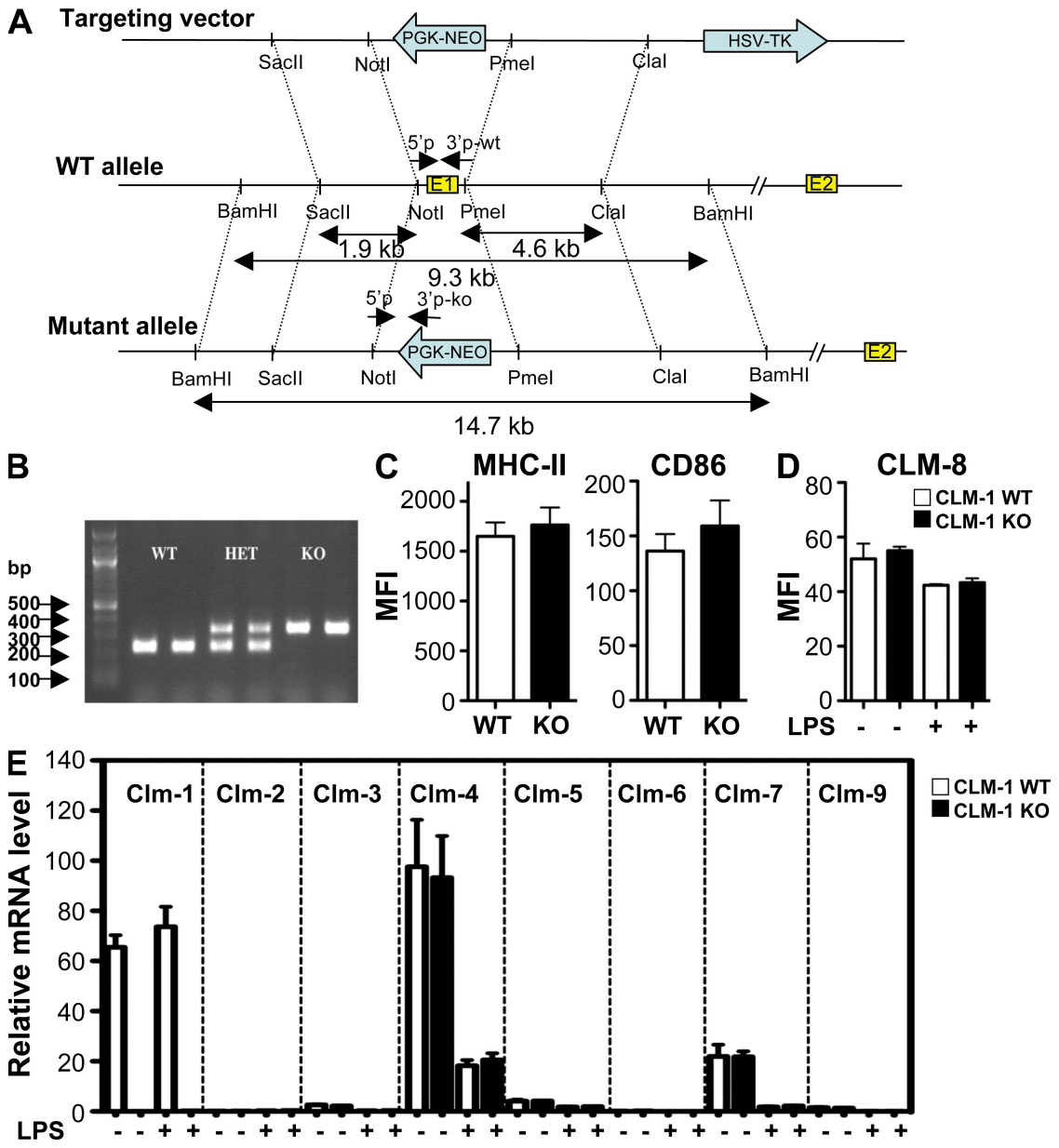

Figure S2. Strategy of targeted disruption of the mouse *Clm-1* gene and expression analysis. (A) Embryonic stem cells with replacement of *Clm-1* exon 1 with the neomycin resistance gene were generated by homologous recombination. The structures of the targeted region of the *Clm-1* gene are shown. E1 and E2 indicate exon 1 and exon 2 of the *Clm-1* gene. (B) PCR screening of genomic DNA obtained from CLM-1 WT, HET, and KO mice. PCR primers are directed against the genomic sequences indicated in A with a common sense primer (5′p) and a WT-specific (3′p-wt) or KO-specific (3′p-ko) antisense primer. (C) Similar levels of MHC-II and CD86 on DCs obtained from CLM-1 WT and KO spinal cords at peak of EAE. MFI, mean fluorescence intensity. Data shown are means ± SEM of three experiments. (D) Similar CLM-8 expression on BMDC derived from CLM-1 WT and KO mice. BMDCs were either unstimulated or stimulated with 100 ng/ml LPS (Sigma-Aldrich) at 37°C for 24 h. CLM-8 expression was analyzed by FACS using a mouse monoclonal anti–CLM-8 antibody. (E) mRNA expression levels of CLM family members in BMDCs obtained from CLM-1 WT and KO mice. Total RNA isolated from BMDCs was analyzed by real-time RT-PCR using verified PCR primer and probe sets (Applied Biosystems). The levels of transcripts were normalized to 18s ribosomal RNA. Data shown in D and E are means ± SEM ($n = 4$).

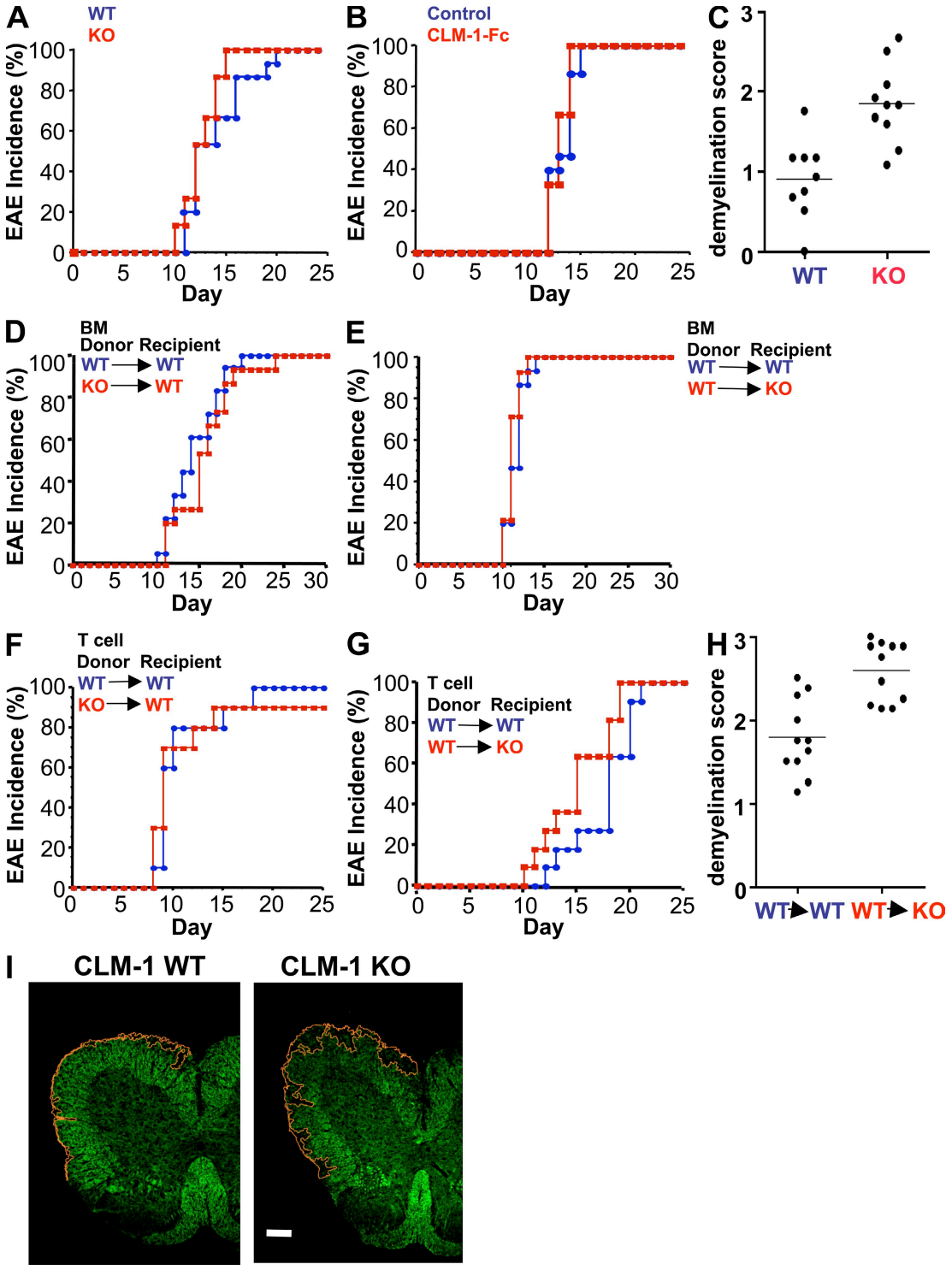

Figure S3. EAE incidence and demyelination in CLM-1 WT and KO mice. (A and B) Disease incidence in CLM-1 WT (A) and KO mice and in C57Bl6 mice (B) treated with CLM-1-Fc or control Fc. (C) Quantification of demyelination in luxol fast blue–stained sections from CLM-1 WT and KO mice based on the following grading: 0, no demyelination; 1, minimal; 2, mild; 3, moderate; 4, marked. Horizontal lines show the means. (D) Disease incidence in irradiated WT mice reconstituted with BM from CLM-1 WT or KO mice. (E) Disease incidence in irradiated CLM-1 WT or KO mice reconstituted with WT BM. (F) Disease incidence in adoptive EAE by transfer of T cells from WT or KO donors into WT recipients. (G) Disease incidence in adoptive EAE by transfer of T cells from WT donors to WT or KO recipients. (H) Demyelination score of G as described in C. Horizontal lines show the means. (I) FluoroMyelin-stained sections taken from the cervical spinal cords of CLM-1 WT and KO mice. The orange outline indicates contiguous areas of demyelination determined by applying intensity thresholds and standard morphological filters as described in the Materials and methods. Bar, 100 µm.

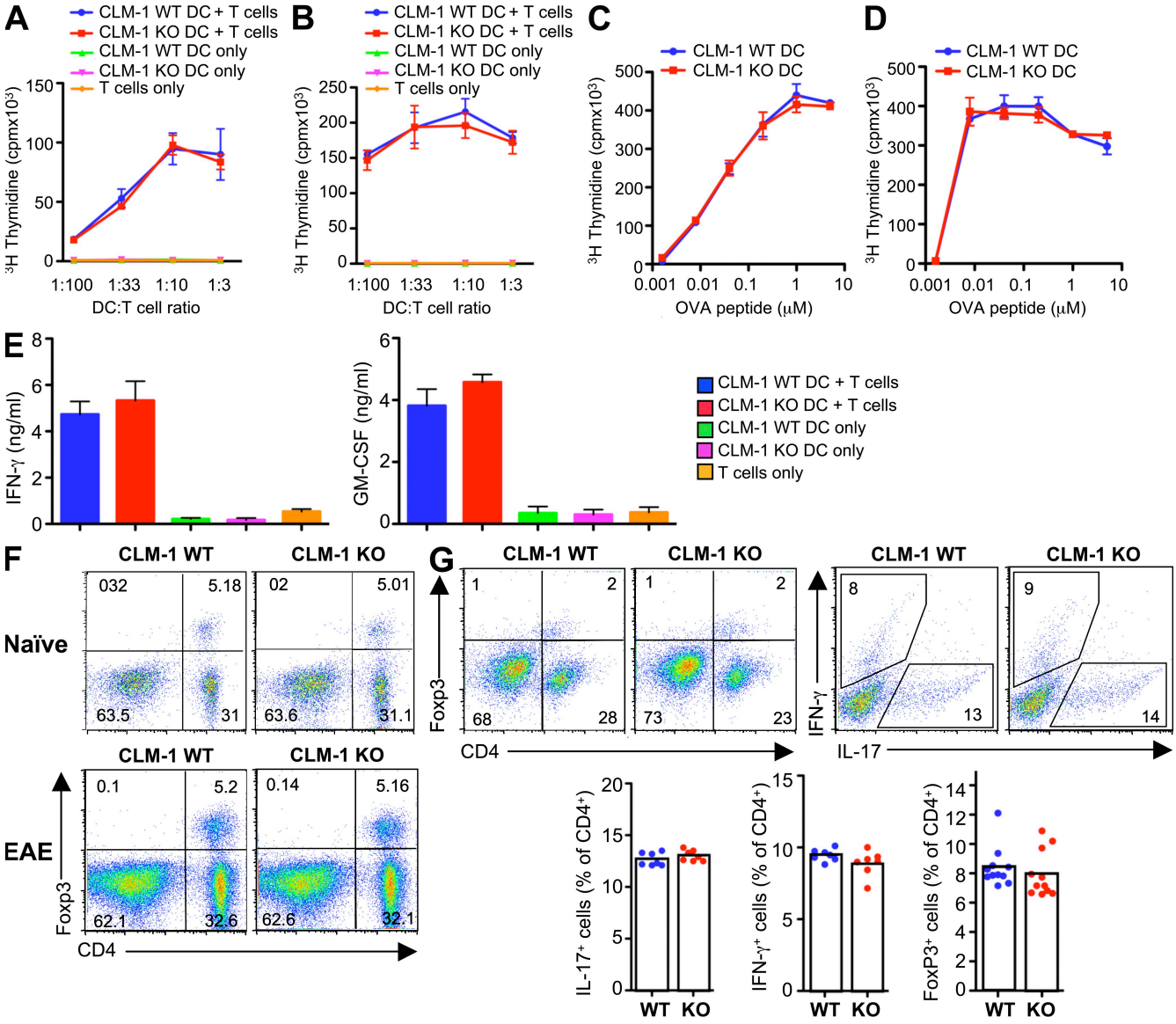

Figure S4. CLM-1 does not influence T cell responses. (A and B) Allogeneic mixed lymphocyte reaction. Sorted splenic DCs (A) or LPS-matured BM-DCs (B) obtained from CLM-1 WT or KO mice on a BALB/c background were co-cultured for 3 d with various ratios of splenic CD4 T cells obtained from mice on a C57BL/6 background. (C and D) Antigen-specific T cell response. Splenic DCs (C) or LPS-matured BMDCs (D) obtained from CLM-1 WT or KO mice were co-cultured with splenic CD4⁺ T cells obtained from DO11.10 T cell transgenic mice for 3 d at DC to T cell ratio of 1:5 in the presence of increasing concentrations of OVA-II peptide (323–339). Proliferation was reflected by the amount of ^{3}H thymidine incorporation. (E) Cytokine production from DO11.10 T cells stimulated with 1 μM (for IFN-γ) or 5 μM (for GM-CSF) OVA-II peptide-pulsed BMDCs from CLM-1 WT or KO mice. (F) CLM-1 does not affect T reg cell generation in peripheral LNs. T reg cells were analyzed by Foxp3 and CD4 staining of DLNs from naive CLM-1 WT and KO mice or from immunized CLM-1 WT and KO mice at peak of EAE. (G) CLM-1 does not influence polarization of T cells and T reg cell generation in the CNS. Th1, Th17, and T reg cells in spinal cords from CLM-1 WT and KO mice at peak of EAE were quantified by intracellular staining of IFN-γ, IL-17, and Foxp3 of CD4 T cells. Each symbol represents one individual mouse. Values in A–E are expressed as means ± SEM (n = 3) and are representative of two (E) or three (A–D) independent experiments.